Surface Modification–Complexation Strategy for Cisplatin Loading in Mesoporous Nanoparticles

ARTICLE *in* JOURNAL OF PHYSICAL CHEMISTRY LETTERS · NOVEMBER 2010

Impact Factor: 7.46 · DOI: 10.1021/jz101483u

THE JOURNAL OF PHYSICAL CHEMISTRY Letters

pubs.acs.org/JPCL

Surface Modification−Complexation Strategy for Cisplatin Loading in Mesoporous Nanoparticles

Jinlou Gu,*,† Shasha Su,† Yongsheng Li,† Qianjun He,‡ Jiaying Zhong,† and Jianlin Shi*,†,‡

†Key Laboratory for Ultrafine Materials of Ministry of Education, School of Materials Science and Engineering, East China University of Science and Technology, Shanghai 200237, China, and ‡The State Key Laboratory of High Performance Ceramics and Superfine Microstructures, Shanghai Institute of Ceramics, Chinese Academy of Sciences, Shanghai 200050, China

ABSTRACT High-density carboxyl groups have been successfully grafted onto the pore surface of mesoporous nanocarriers which served to complex with platinum atoms in cisplatin, leading to much increased drug loading efficiency, distinctly prolonged and pH-responsive cisplatin release, and greatly enhanced growth inhibition effect against MCF-7 and HeLa cancer cell lines.

SECTION Nanoparticles and Nanostructures

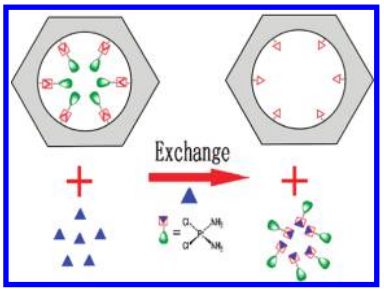

Cisplatin (*cis*-dichlorodiammineplatinum(II), CDDP) is one of the most effective and widely applied antineoplastic agents with therapeutic activity against a wide variety of cancers.[1,2] However, the clinical usefulness of CDDP is often restricted by the development of drug resistance and systemic toxicity.[3,4] To counteract the resistance, generally, clinical dosing of CDDP is elevated to higher levels, which will, however, inevitably cause systemic toxicity.[5−7] As such, a drug delivery system (DDS) that can enhance CDDP accumulation in the tumor in order to achieve enhanced antitumor activity as well as reduced cytotoxicity is highly desirable.[8−11]

Recently, mesoporous silica nanoparticles (MSNs) have been used as anticancer drug delivery vehicles, taking their several advantages over traditional systems.[12−16] The prominent surface area and large pore volume of MSNs allow for loading vast amounts of drugs. Their pore size and shape could be facilely tuned to satisfy different kinds of drugs storage.[17−19] Additionally, it has been previously demonstrated that MSNs possess "noncytotoxic" properties and are able to escape the endolysosomal entrapment.[20,21] Therefore, the MSNs could serve not only as vehicles for incorporating drug molecules that are not water-soluble or easily membrane-transportable and deliver them into cells, but they could also protect them from being damaged.

MSNs contain abundant silanol groups (Si−OH) on the pore surface, which can be further functionalized by different ionic functional groups in order to create favorable surface−drug interactions and, in turn, enhance adsorption capacity for anticancer drugs.[22] It has been well documented that CDDP is very active to form a complex with carboxylic acid terminal groups by replacing the chloride ion ligands, as shown in Scheme 1.[5−7] Therefore, large amount of CDDP anticancer drug could be bonded into the pore channels of MSNs via ligand exchange if high-density carboxyl groups can be introduced in advance.

However, in traditional surface functionalization of MSNs via postgrafting,[23] the organic moieties often congregated more on the pore channel openings, and the grafting amount was thus limited due to the partial pore blocking, which resulted in a much decreased drug loading amount. The cocondensation method[24] produced better control over the loading and distribution of the organic groups but generally at the expense of the mesoscopic ordering. Furthermore, this method also made an important fraction of the functional groups inaccessible and/or embedded in the silica network. Motivated by the existing drawbacks of the two general routes, herein, we modified MSNs with high-density carboxyl groups homogeneously coated on the pore surface, as demonstrated in Scheme 2. A large amount of hydroxyl groups was grown directly from the surface silanol groups by utilizing a highly reactive, nonbulky monomer of glycidol, which was subsequently esterified to link the carboxyl moieties.[25] In this way, favorable carboxyl−drug interactions finally dramatically increased the adsorption capacity and efficiency for CDDP and distinctly prolonged the delivery.

The parent MSNs were prepared by a surfactant-templated, base-catalyzed condensation procedure, as reported (see Supporting Information).[26,27] SEM and TEM images (Figure S1 and S2, Supporting Information) show that the spherical MSNs have a uniform diameter of ∼100 nm, and no morphology change is found upon grafting of the carboxyl groups. Besides, the ∼2.5 nm in diameter mesopore channels cross through the whole area of the nanoparticles, which facilitates the access of guest molecules. The small-angle XRD was applied to monitor the ordering evolvement of MSNs and carboxylic-acid-modified MSNs (Figure S3, Supporting Information). Both samples exhibit hexagonally ordered structures with (100), (110), and (200) reflections, indicating that the ordered structure of the parent MSNs was reasonably maintained after the conjugation with carboxyl groups.

We employed IR spectra and ^{13}C solid NMR to track the grafting process in depth because the success in installing high-density carboxyl groups onto MSNs is the key to the

Received Date: November 1, 2010
Accepted Date: November 29, 2010
Published on Web Date: November 30, 2010

DOI: 10.1021/jz101483u | *J. Phys. Chem. Lett.* **2010**, *1*, 3446–3450

Scheme 1. Proposed Complexation Process for CDDP and Carboxyl Groups in the Mesochannels of MSNs

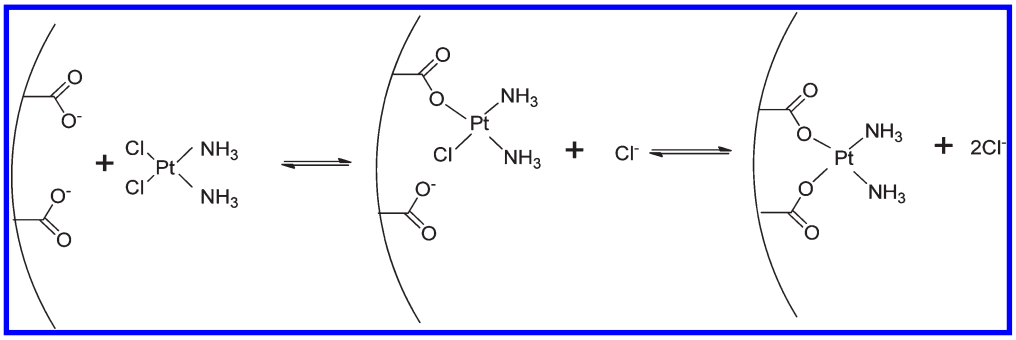

Scheme 2. Functionalization Procedures for the As-Synthesized MSNs with Carboxylic Acid Groups in Two Steps

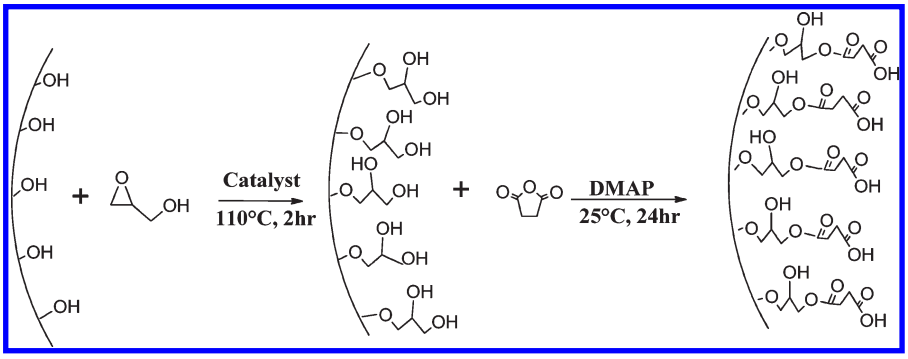

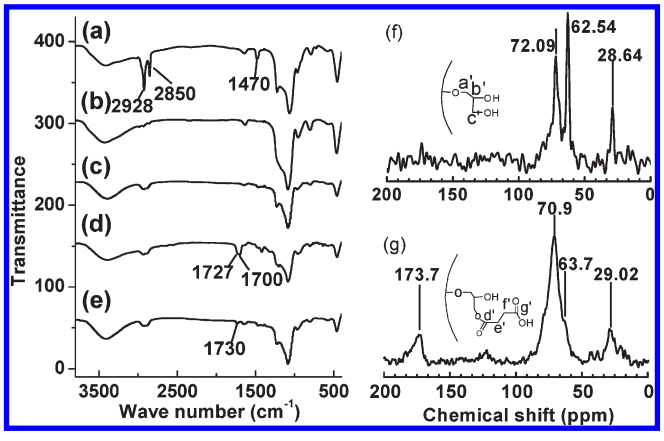

Figure 1. FT-IR spectra of MSNs before (a) and after (b) surfactant extraction and hydroxyl groups functionalized (c), carboxyl groups functionalized (d), and carboxyl groups functionalized with loaded CDDP (e). The ^{13}C solid NMR spectra of MSNs modified with hydroxyl groups (f) and carboxyl groups (g).

subsequent loading of CDDP. Before extraction, the large amount of surfactant in the MSNs gives the characteristic C−H vibration bands at 2850−2930 cm^{-1} and C−H deformation bands at ∼1470 cm^{-1} (Figure 1a). After extraction of surfactant, all IR peaks from CTAB molecules disappear (Figure 1b).[28] However, the hydroxyl-functionalized MSNs (MSN−OH) show the C−H mode at 2850−2930 cm^{-1} again (Figure 1c). The ^{13}C solid NMR spectrum of MSN−OH (Figure 1f) shows signals at 28.6, 62.5, and 72.1 ppm, which are assigned to a′, b′, and c′ position carbons. These results indicate that the hydroxyl groups were successfully modified in the framework of MSNs by covalently bonding via reaction between Si−OH groups of the extracted MSNs and oxirane rings of glycidol.[25] The two IR absorption peaks for MSN−COOH (Figure 1d) at 1727 and 1700 cm^{-1} clearly indicate the presence of terminal carboxyl groups. Meanwhile, in the ^{13}C solid NMR spectrum of MSN−COOH (Figure 1g), the broadened peak at 173.7 ppm attributed to the d′ and g′ position carbons also confirms the success in fixing carboxylic acid terminal groups onto the surface of the synthesized MSNs via an ester linkage.[19] The IR spectrum of MSN−COOH after reaction with CDDP solution (MSN−COOH−CDDP) (Figure 1e) shows that the COO$^-$ stretching vibration of MSN−COOH at 1700 cm^{-1} has decreased. This illustrates that some of the −COOH groups in the MSNs were spontaneously bonded to Pt atoms from CDDP via a ligand exchange reaction[5] with the chloride ions in CDDP, as demonstrated in Scheme 1. Due to this strategetic modification process, high-density carboxyl groups were efficiently introduced into the mesochannels and subsequently interacted with CDDP. The specific density was calculated by TGA and titration measurements, and the value was up to ∼0.953 carboxyl groups nm^{-2} by TGA analysis (Figure S4, Supporting Information). It was found that the loading efficiency of CDDP in the current MSNs was up to 95%, and the drug loading capacity was reasonably high up to 20% as compared to the usually low drug loading capacity, as reported in the literature[16] (Figure S5 and experimental details in Supporting Information).

The nitrogen adsorption curves (Figure S6a, Supporting Information) reveal type-IV isotherms with sharp capillary condensation steps for all of the samples before and after the

DOI: 10.1021/jz101483u | J. Phys. Chem. Lett. 2010, 1, 3446–3450

grafting and loading process. This demonstrates the presence of mesoporous structure in these materials and also indicates that the modification process did not destroy the structural integrity of the parent MSNs. The pore sizes of MSN−COOH and MSN−COOH−CDDP (Figure S6b, Supporting Information) decrease to 2.43 and 2.40 nm from ∼2.62 nm of the parent MSNs, respectively, and the pore volume and surface area decrease with the similar trends, as summarized in Table 1. The decent decreases in the surface area and pore volume may have resulted from the drug molecule bonding in the mesochannels of MSN−COOH samples via ligand exchanges.

The drug release profile is of great importance in applying the synthesized systems to a practical drug delivery for cancer chemotherapy. The release of CDDP from MSNs was extraordinarily sustained as compared to the free drugs in dialysis bags in PBS with pHs from 4 to 7.4, as shown in Figure 2a. This is quite beneficial to prevent the drug dissipation before reaching the tumor tissues.[29] The MSN−drug conjugate released CDDP by a ligand exchange reaction between the chloride ions in PBS and carboxyl groups of the MSNs, as demonstrated in Scheme 1. The whole release profile demonstrates the sustained properties without a burst release effect within the first 24 h, which was almost inevitably present in the traditional DDSs.[8−11] This is important for reducing the trapped drug leakage and for protecting CDDP from inaction in the physiological environment prior to its reaching the target cells. As a control experiment, we found that the release rate of free CDDP from dialysis bag was up to 97.3% in 10 h. The carboxyl−drug complexion and the slow drug diffusion from the mesochannels to the media solution should be responsible for the sustained release characteristics.[30] It takes about as long as 13 days for the CDDP to release from the synthesized DDS to saturate in PBS solutions.

Table 1. Structure Parameters of the Parent and Modified MSNs

samples	S_{BET} (m^2/g)	D_{BJH} (nm)	V_P (cm^3/g)
MSNs	1040	2.62	1.12
MSN−COOH	886	2.43	0.72
MSN−COOH−CDDP	621	2.40	0.51

It is very interesting to note that the drug release is acid-dependent. At pH = 5.5, about 85% of CDDP is released from the nanocarriers after 320 h, while at pH = 7.4, the amount is reduced to less than 60% within the same time duration. It can be more clearly found from Figure 2b, with an enlarged scale for the first 24 h, that lower pH conditions accelerated the release of the drugs. Because carboxylic acid is a weak electrolyte, the pH will affect its dissociation constant and therefore change its coordination ability with Pt atoms in CDDP, which should be responsible for the pH-responsive properties of the obtained DDS. This would allow for the minimization of the amount of drug leaching out of MSNs during their circulation in the blood with a pH of 7.4 and enable a large amount of intracellular drug release once the nanocarriers are taken inside of the target cells through endocytosis because endosome/lysosome has a low pH of ∼5.[14]

Cellular uptake of the synthesized MSNs loaded with CDDP was examined by direct TEM observation. The MCF-7 cells were incubated with 200 μg/mL of MSNs for 24 h. Then, the cells were washed twice with D-hanks and harvested by incubation with 0.25% trypsin for 5 min. After that, the MFC-7 cells were fixed by glutaraldehyde at room temperature. Ultrathin sections of approximately 70 nm thickness were cut with a diamond knife on a Leica UC6 ultramicrotome and transferred to the copper grid (see experiments in Supporting Information for details). From the TEM image of Figure 3a, we can clearly find that the MSNs have crossed the cell membrane. However, they did not penetrate the nuclear membrane; instead, they accumulated in cytoplasm. As marked by the red circle in Figure 3a, intracellular endosomes have visibly formed after the uptake of the MSNs by MCF-7 cells, implying a possible receptor-mediated endocytotic process.[17] The morphology of the MCNs is maintained, as shown in the enlarged TEM image (Figure 3b). These reveal that drug complexes of CDDP@MCNs could be effectively internalized into living cells.

To test the therapeutic effect of the synthesized MSN−COOH−CDDP, we studied the cytotoxicity of the synthesized samples against MCF-7 and HeLa cell lines using an MTT method (see Supporting Information). From the top black

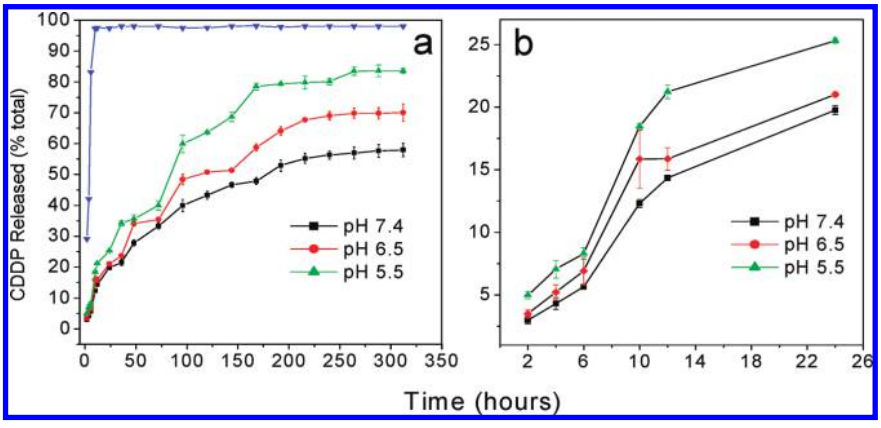

Figure 2. (a) Free CDDP release profile from the dialysis bags (blue line) and pH-dependent CDDP release from MSNs in PBS buffer at 37 °C. (b) Enlarged curves for the first 24 h release profile.

DOI: 10.1021/jz101483u | J. Phys. Chem. Lett. 2010, 1, 3446–3450

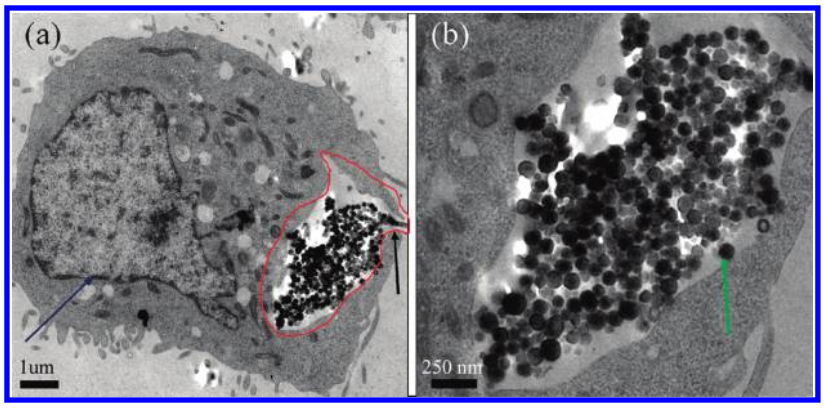

Figure 3. TEM image of MCF-7 cells after incubation with CDDP@MSNs at the concentration of 200 μg/mL and 37 °C for 24 h (a); the blue arrow marks the nucleus, and the red curve circles the internalized MSNs. The enlarged TEM image (b) demonstrates the ordered MSNs, marked by the green arrow.

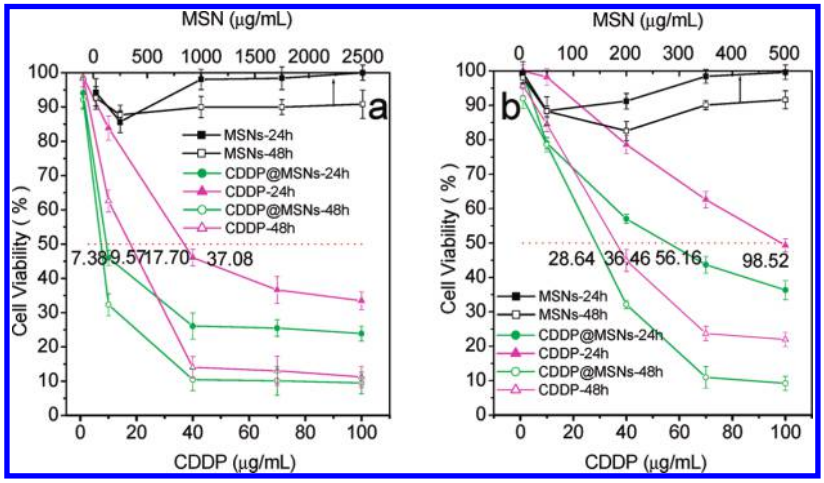

Figure 4. Comparative cytotoxicity profiles of free CDDP (purple), MSN−COOH−CDDP (green), and parent MSNs (black) against HeLa cell lines (a) and MCF-7 cells (b) after culture for 1 and 2 days. The top abscissa is for the parent MSNs, while the bottom one is for free CDDP and MSN−COOH−CDDP.

lines in Figure 4, it can be found that parent MSNs themselves are almost noncytotoxic to both cell lines tested, indicating good biocompatibility of the MSNs, in agreement with the reported results.[18,26] Growth inhibition and killing of both human cancer cells could be clearly observed when the cells were treated with either the suspension of MSN−COOH−CDDP or a solution of free CDDP. The synthesized MSN−COOH−CDDP demonstrated a dose-dependent cytotoxic effect both in MCF-7 and HeLa cells. Meanwhile, it showed a substantial increase in the cytotoxicity relative to the free CDDP in 2 days when compared on a per platinum basis, and these phenomena were more significant in HeLa cell lines (Figure 4a and b). Half-maximal inhibitory concentrations (IC_{50}) for day 1 and day 2 were determined from cell survival diagrams and are labeled in Figure 4. The IC_{50} values of MSN−COOH−CDDP after 1 or 2 days of incubation were less than that of free CDDP both in HeLa and MCF-7 cell lines. This suggested that the anticancer drug of CDDP was successfully delivered via the prepared MSN−COOH−CDDP and subsequently released within the cancer cells and more effectively inhibited the growth of the cancer cell lines applied.[26]

In summary, high-density carboxyl groups were grafted onto the mesopore surface of MSNs to serve as effective ligands for the linking of Pt atoms from the CDDP anticancer drug. Due to those strong interactions, extraordinarily high CDDP loading efficiency up to 95% in MSNs was achieved, and the loaded CDDP showed a pH-responsive and greatly sustained release in PBS buffer for over 13 days. The MSN−COOH−CDDP had a higher antitumor efficiency than free CDDP against both MCF-7 and HeLa cell lines. These results justify the suitability of the functionalized MSNs for the sustained release and controlled delivery of CDDP to the target cells.

SUPPORTING INFORMATION AVAILABLE

Experiement details and TEM, SEM, XRD, BET, UV, and TG analysis figures. This material is available free of charge via the Internet at http://pubs.acs.org.

AUTHOR INFORMATION

Corresponding Author:

*To whom correspondence should be addressed. E-mail: jinlougu@ecust.edu.cn (J.G.); jlshi@mail.sic.ac.cn (J.S.).

DOI: 10.1021/jz101483u | J. Phys. Chem. Lett. 2010, 1, 3446–3450

ACKNOWLEDGMENT This work was financially supported by the Shanghai Pujiang Program (No. 09PJ1403000), the Research Fund for the Doctoral Program of Higher Education (No. 20090074120009), and the Natural Science Foundation of China (No. 51072053).

REFERENCES

(1) Aryal, S.; Jack Hu, C. M.; Zhang, L. F. Polymer−Cisplatin Conjugate Nanoparticles for Acid-Responsive Drug Delivery. *ACS Nano* **2010,** *4*, 251–258.

(2) Bhirde, A. A.; Patel, V.; Gavard, J.; Zhang, G.; Sousa, A. A.; Masedunskas, A.; Leapman, R. D.; Weigert, R. J.; Gutkind, S.; Rusling, J. F. Targeted Killing of Cancer Cells in Vivo and in Vitro with EGF-Directed Carbon Nanotube-Based Drug Delivery. *ACS Nano* **2009,** *3*, 307–316.

(3) Dhar, S.; Daniel, W. L.; Giljohann, D. A.; Mirkin, C. A.; Lippard, S. J. Polyvalent Oligonucleotide Gold Nanoparticle Conjugates as Delivery Vehicles for Platinum(IV) Warheads. *J. Am. Chem. Soc.* **2009,** *131*, 14652–14653.

(4) Dhar, S.; Gu, F. X.; Langer, R. O.; Farokhzad, O. C.; Lippard, S. J. Targeted Delivery of Cisplatin to Prostate Cancer Cells by Aptamer Functionalized Pt(IV) Prodrug−PLGA−PEG Nanoparticles. *Proc. Natl. Acad. Sci. U.S.A.* **2008,** *105*, 17356–17361.

(5) Haxton, K. J.; Burt, H. M. Hyperbranched Polymers for Controlled Release of Cisplatin. *Dalton Trans.* **2008,** *37*, 5872–5875.

(6) Ajima, K.; Yudasaka, M.; Maigne, A.; Miyawaki, J.; Iijima, S. Effect of Functional Groups at Hole Edges on Cisplatin Release from Inside Single-Wall Carbon Nanohorns. *J. Phys. Chem. B* **2006,** *110*, 5773–5778.

(7) Xu, P. S.; Kirk, E. A. V.; Murdoch, W. J.; Zhan, Y. H.; Isaak, D. D.; Radosz, M.; Shen, Y. Q. Anticancer Efficacies of Cisplatin-Releasing pH-Responsive Nanoparticles. *Biomacromolecules* **2006,** *7*, 829–835.

(8) Cheng, K.; Peng, S.; Xu, C.; Sun, S. Porous Hollow Fe_3O_4 Nanoparticles for Targeted Delivery and Controlled Release of Cisplatin. *J. Am. Chem. Soc.* **2009,** *131*, 10637–10644.

(9) Xu, C.; Wang, B.; Sun, S. Dumbbell-like Au−Fe_3O_4 Nanoparticles for Target-Specific Platin Delivery. *J. Am. Chem. Soc.* **2009,** *131*, 4216–4217.

(10) Rieter, W. J.; Pott, K. M.; Taylor, K. M. L.; Lin, W. Nanoscale Coordination Polymers for Platinum-Based Anticancer Drug Delivery. *J. Am. Chem. Soc.* **2008,** *130*, 11584–11585.

(11) Dhar, S.; Liu, Z.; Thomale, J.; Dai, H. J.; Lippard, S. J. Targeted Single-Wall Carbon Nanotube-Mediated Pt(IV) Prodrug Delivery Using Folate as a Homing Device. *J. Am. Chem. Soc.* **2008,** *130*, 11467–11476.

(12) Roseholm, J.; Sahlgren, C.; Linden, M. Cancer-Cell Targeting and Cell-Specific Delivery by Mesoporous Silica Nanoparticles. *J. Mater. Chem.* **2010,** *20*, 2707–2713.

(13) Vivero-Escoto, J. L.; Slowing, I. I.; Lin, S. Y. Tuning the Cellular Uptake and Cytotoxicity Properties of Oligonucleotide Intercalator-Functionalized Mesoporous Silica Nanoparticles with Human Cervical Cancer Cells HeLa. *Biomaterials* **2010,** *31*, 1325–1333.

(14) Rosenholm, J. M.; Peuhu, E.; Erikson, J. E.; Sahlgren, C.; Linden, M. Targeted Intracellular Delivery of Hydrophobic Agents Using Mesoporous Hybrid Silica Nanoparticles as Carrier Systems. *Nano Lett.* **2009,** *9*, 3308–3311.

(15) Tsai, C. P.; Chen, C. Y.; Hung, Y.; Chang, F. H.; Mou, C. Y. Monoclonal Antibody-Functionalized Mesoporous Silica Nanoparticles (MSN) for Selective Targeting Breast Cancer Cells. *J. Mater. Chem.* **2009,** *19*, 5737–5743.

(16) Lu, J.; Liong, M.; Zink, J. I.; Tamanoi, F. Mesoporous Silica Nanoparticles as a Delivery System for Hydrophobic Anticancer Drugs. *Small* **2007,** *3*, 1341–1346.

(17) Tao, Z.; Toms, B.; Goodisman, J.; Asefa, T. Mesoporous Silica Microparticles Enhance the Cytotoxicity of Anticancer Platinum Drugs. *ACS Nano* **2010,** *4*, 789–794.

(18) Lu, F.; Wu, S. H.; Hung, Y.; Mou, C. Y. Size Effect on Cell Uptake in Well-Suspended, Uniform Mesoporous Silica Nanoparticle. *Small* **2009,** *5*, 1408–1413.

(19) Gu, J.; Fan, W.; Shimojima, A.; Okubo, T. Organic−Inorganic Mesoporous Nanocarriers Integrated with Biogenic Ligands. *Small* **2007,** *3*, 1740–1744.

(20) Lee, J. E.; Lee, N.; Kim, H.; Kim, J.; Choi, S. H.; Kim, J. H.; Kim, T.; Song, I. C.; Park, S. P.; Moon, W. K.; et al. Uniform Mesoporous Dye-Doped Silica Nanoparticles Decorated with Multiple Magnetite Nanocrystals for Simultaneous Enhanced Magnetic Resonance Imaging, Fluorescence Imaging and Drug Delivery. *J. Am. Chem. Soc.* **2010,** *132*, 552–557.

(21) Trewyn, B. G.; Giri, S.; Slowing, I. I.; Lin, V. S. Y. Mesoporous Silica Nanoparticle Based Controlled Release, Drug Delivery, and Biosensor Systems. *Chem. Commun.* **2007,** *43*, 3236–3245.

(22) Rosenholm, J. M.; Meinander, A.; Penhu, E.; Niemi, R.; Eriksson, J. E.; Sahlgren, C.; Linden, M. Targeting of Porous Hybrid Silica Nanoparticles to Cancer Cells. *ACS Nano* **2009,** *3*, 197–206.

(23) Rosenholm, J. M.; Linden, M. Wet-Chemical Analysis of Surface Concentration of Accessible Groups on Different Amino-Functionalized Mesoporous SBA-15 Silicas. *Chem. Mater.* **2007,** *19*, 5023–5034.

(24) Kecht, J.; Schlossbauer, A.; Bein, T. Selective Functionalization of the Outer and Inner Surfaces in Mesoporous Silica Nanoparticles. *Chem. Mater.* **2008,** *20*, 7207–7214.

(25) Liu, Y. L.; Hsu, C. Y.; Wang, M. L.; Chen, H. S. A Novel Approach of Chemical Functionalization on Nano-scaled Silica Particles. *Nanotechnology* **2003,** *14*, 813–819.

(26) Lai, C. Y.; Trewyn, B. G.; eftinija, D. M.; Jeftinija, J K.; Xu, S.; Jeftinija, S.; V. Lin, S. Y. A Mesoporous Silica Nanosphere-Based Carrier System with Chemically Removable CdS Nanoparticle Caps for Stimuli-Responsive Controlled Release of Neurotransmitters and Drug Molecules. *J. Am. Chem. Soc.* **2003,** *125*, 4451–4459.

(27) Cai, Q.; Luo, Z. S.; Pang, W. Q.; Fan, Y. W.; Chen, X. H.; Cui, F. Z. Dilute Solution Routes to Various Controllable Morphologies of MCM-41 Silica with a Basic Medium. *Chem. Mater.* **2001,** *13*, 258–263.

(28) Gu, J. L.; Fan, W.; Shimojima, A.; Okubo, T. Microwave-Induced Synthesis of Highly Dispersed Gold Nanoparticles within the Pore Channels of Mesoporous Silica. *J. Solid State Chem.* **2008,** *181*, 957–963.

(29) Prabahara, M.; Grailer, J. J.; Pilla, S.; D. Steeber, A.; Gong, S. Gold Nanoparticles with a Monolayer of Doxorubicin Conjugated Amphiphilic Block Copolymer for Tumor-Targeted Drug Delivery. *Biomaterials* **2009,** *30*, 6065–6075.

(30) Zhao, W. R.; Gu, J. L.; Zhang, L. X.; Chen, H. R.; Shi, J. L. Fabrication of Uniform Magnetic Nanocomposite Spheres with a Magnetic Core/Mesoporous Silica Shell Structure. *J. Am. Chem. Soc.* **2005,** *127*, 8916–8917.

DOI: 10.1021/jz101483u | *J. Phys. Chem. Lett.* **2010,** *1*, 3446–3450